Seeding, Controlling, and Benefiting from the Microbunching Instability

S. Seletskiy, B. Podobedov, Y. Shen, and X. Yang

Phys. Rev. Lett. **111**, 034803 — Published 19 July 2013

DOI: 10.1103/PhysRevLett.111.034803

Seeding, controlling and benefiting from microbunching instability

S. Seletskiy, B. Podobedov, Y. Shen, X. Yang
National Synchrotron Light Source, Brookhaven National Laboratory, Upton, NY 11973, U.S.A.

Advanced light sources using relativistic electrons rely on coherent emission from high-density (compressed) beams. These beams, typically produced by photo-injected linear accelerators, can suffer from uncontrolled microbunching instabilities that are difficult to manage since a complete understanding of their growth due to space-charge and other wakefields is lacking. Here we present the first systematic measurements of microbunching instability using electron beams pre-modulated in a controlled fashion. By comparing beams having various modulation depths and wavelengths with unmodulated beams, we are able to benchmark, for the first time, the analytical calculations for the microbunching instability. In addition, our results give a proof of principle demonstration of a Longitudinal Space Charge Amplifier (LSCA) where a specific beam density pattern develops and grows. A potential application of this particular LSCA scheme is for controlling waveforms and enhancing the spectral content of linac-based sources of coherent terahertz radiation.

PACS numbers: 29.27.Bd, 29.27.Fh, 41.60.Cr, 41.75.Ht

The linear accelerators, commonly used as injectors, for short wavelength free electron lasers (FELs) [1, 2] utilize bunch compressors (BC) [2, 3] for producing electron bunches having both high charge and subpicosecond length. A typical BC reduces the lengths of individual bunches in a bunched electron beam by inducing a well-defined correlation between the energy and longitudinal position of an electron in the bunch (energy chirp). This chirped bunch is then directed through a dedicated dispersive region formed by a set of dipole magnets. The dispersion correlates electron energy with path length such that higher energy electrons in the bunch tail travel a shorter distance and catch up to lower energy electrons at the front. The method is analogous to compression of a chirped laser pulse.

Upstream of the BC, a longitudinal space charge (LSC) wakefield, as well as other wakefields, can convert small initial beam density modulations into additional (and usually unwanted) energy modulations; these, in turn, are transformed into density modulations of greater amplitude in the BC dispersive region. This process degrades FEL performance [4] by increasing the fragmentation of the beam in longitudinal phase space (i.e. modulation of the electron density in both real-space and energy coordinates) and is known as microbunching instability [5–8].

In recent years the microbunching instability has been the subject of intense studies. It was shown that, depending on the design of the FEL injector, both shot noise [9] and longitudinal intensity variations of the photocathode laser [3] can be an initial source of density modulations that lead to microbunching. As a remedy against this particular instability mechanism, a so-called laser heater [10, 11] was shown to suppress the microbunching to a reasonable level [4]. Some of the recent developments regarding the microbunching instability include theoretical exploration of accelerator lattices that naturally suppress microbunching [12], experimental demonstration of a possibility to eliminate microbunching instability from a typical FEL injector with single stage bunch compressor (and operating without a laser heater) by utilizing a longitudinally smooth photocathode laser [3], and a suggestion to actually exploit the microbunching effect to subsequently generate coherent VUV and X-Ray radiation [13]. This last suggestion is based on the fact that the described microbunching instability mechanism constitutes the LSC amplifier (LSCA) with a large relative bandwidth.

Despite advances in understanding and controlling the microbunching instability, direct benchmarking of the model for microbunching gain has been missing. We present the first direct measurement of microbunching gain performed at the Source Development Laboratory (SDL) at the National Synchrotron Light Source. We also experimentally demonstrate, for the first time, the feasibility of the LSCA idea, and show its potential application to the enhancement of the linac-based tunable terahertz (THz) source [14]. Preliminary results of our work were reported in [15].

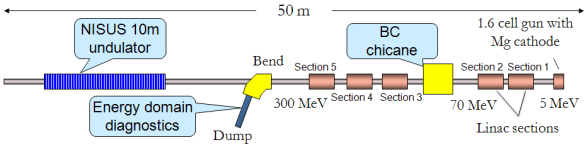

FIG. 1: The SDL layout. The gun and the first two linac tanks are powered by a single klystron.

At the SDL [2] an electron bunch generated in the photocathode RF gun is accelerated to 70 MeV, utilizing two SLAC type traveling-wave linear accelerator sections. The RF phase for one section is set for off-crest acceleration to produce the energy chirp. The chirped bunch is then compressed in a four-bend dipole chicane, that provides relevant dispersion. Three more linac sections follow after the BC to further accelerate the electron beam to a maximum 300 MeV final energy. After acceleration, the beam passes through a 10 m long undulator to produce coherent radiation from IR to XUV

wavelengths. The SDL beamline is equipped with a spectrometer magnet located downstream of the bunch compressor, followed by a beam profile monitor (BPM). This spectrometer can be utilized to obtain beam temporal profile as well as its energy spectrum. For the former one can use RF zero-phasing method [3]. The electron beam is energy chirped by one of the linac sections set to the nonaccelerating (zero) phase, and then it is dispersed by a dipole magnet, so that the different time slices of the beam are projected on the scintillating screen at different positions. This method yields an RMS time resolution of about 7 fs [3].

The photocathode RF gun is illuminated by 266 nm light pulses from a frequency tripled Ti:sapphire laser system synchronized to the linac RF. This system consists of an oscillator producing a train of 100 fs pulses at 800nm followed by a chirped pulse amplifier and harmonic generation to 266 nm. Fig. 1 schematically shows the SDL layout.

At the SDL linac, the microbunching instability is known to be dominated by the longitudinal space charge (LSC) [3]. The LSC converts initial beam density modulation characterized by the wavenumber k and the bunching factor $b(k)$ into energy modulation of amplitude $\Delta\gamma(k)$. The latter is converted back to the density modulation with a bunching factor $b_f(k/C)$ in the BC chicane, where $C = 1/(1 + hR_{56})$ is the compression ratio, h is the beam chirp, and R_{56} is the chicane compaction factor. The gain is given by [7]:

$$G(k) = \frac{b_f(k/C)}{b(k)} = \left| CkR_{56}\frac{\Delta\gamma(k)}{\gamma b(k)} \right| \cdot e^{-\frac{(CkR_{56}\sigma_E)^2}{2E^2}} \quad (1)$$

where $\gamma = E/mc^2$, m is the mass of the electron, E is the beam energy, and σ_E is the uncorrelated energy spread. The energy modulation at the end of the linac of length L is:

$$\Delta\gamma(k) = -\frac{4\pi I}{Z_0 I_A}\int_0^L Z(k,z)b(k,z)\,dz \quad (2)$$

where Z is LSC impedance, $Z_0 \approx 377\ \Omega$ is the free-space impedance, I is the beam current, and $I_A \approx 17$ kA is the Alfven current.

The microbunching gain in Eq. 1 is derived under the assumption that the final modulation is much larger than the initial one, and therefore is only applicable in the linear regime. It can be used as long as modulation wavelength is small in comparison to bunch length.

In this paper we find the microbunching gain by taking the ratio of measured amplitudes of density modulation of the compressed and uncompressed bunches. The electron bunch density must be modulated in a controlled fashion in amplitude with easily tuned frequency. Since photoelectron emission from the cathode is prompt with respect to the laser light, the temporal characteristics of the laser pulse primarily determine the longitudinal distribution of the electron bunch. Moreover, due to the naturally small microbunching gain at the SDL [3], the initial microbunching is determined by the laser-induced modulation of the bunch density rather than by shot noise.

To produce the longitudinally modulated laser pulse used in our experiment, we employ a technique described in [14, 16]. Thus, we chirp the 266 nm laser pulse to 6 ps (FWHM) using a grating pair, and then split the chirped pulse into two pulses. One pulse is delayed by a variable interval, τ, with respect to the other. Thereafter, the two chirped pulses are recombined. The electric field of a linearly chirped optical pulse with a Gaussian envelope is:

$$E(t) = E_0 \exp(-\alpha t^2)\exp(i(\omega_0 t + bt^2)) \quad (3)$$

where E_0 is the amplitude, ω_0 is the carrier frequency, $1/\sqrt{\alpha}$ is the pulse duration and b is the chirp rate. A superposition of this chirped pulse with its time-shifted replica leads to the output pulse:

$$\begin{aligned} I(t,\tau) &= |E(t) + E(t+\tau)|^2 = I(t) + I(t+\tau) \\ &+ 2\sqrt{I(t)I(t+\tau)}\cos(\omega_0\tau + b\tau^2 + 2b\tau t) \end{aligned} \quad (4)$$

The time difference between these two pulses produces a beat frequency, $\mu = 2b\tau$, that is directly proportional to the time delay, τ, and the frequency chirp rate b. Therefore, the resultant output pulse has a Gaussian envelope modulated by a cosine function with a center frequency of $2b\tau$, that is easily tuned by varying the time delay or the frequency chirp of the input pulses.

Prior to describing our measurements an important remark is in order. As was noted by others (see i.e. [17]) beam density modulation measurements by the standard zero-phasing method could be compromised in cases of significant energy modulation present, because the energy modulation could mask the density modulation. To exclude this possibility, for each set of parameters our zero-phasing measurements were performed at two opposite zero-crossing phases, and the resulting density modulation depth was confirmed to remain the same within the measurement accuracy. To further rule-out possible effects of energy modulation, we checked that increasing the zero-phasing amplitude did not affect the depth of the modulation observed.

Fig. 2 depicts an example of a 90 pC 70 MeV electron beam produced by the longitudinally modulated photocathode laser; the background noise of a few percent was removed from the image (to do this, we fitted the histogram of image intensity distribution with a Gaussian, and subtracted from the image the intensity level of the maximum plus one sigma of the fit). It was checked that the measured gain uncertainty associated with background subtraction was insignificant, a 1 % at most. The zero-phasing measurement of the given beam gives the induced modulation wavelength of about 60 μm. According to Eq. 1, we expect to see amplification of microbunching at wavelengths $\lambda \geq 30$ μm (the BC R_{56} is 54 mm, the measured relative uncorrelated energy spread of the beam is about $1.5 \cdot 10^{-4}$) at the BC compression factor

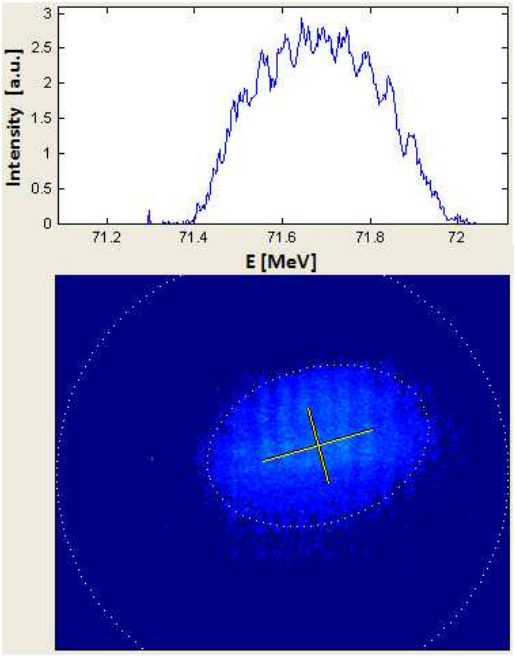

FIG. 2: The zero phasing of the 90 pC beam produced by the longitudinally modulated photocathode laser. The horizontal axis gives spectrometer readings in MeV. The vertical axis shows amplitude in arbitrary units. The wavelength of the induced modulation is about 60 μm.

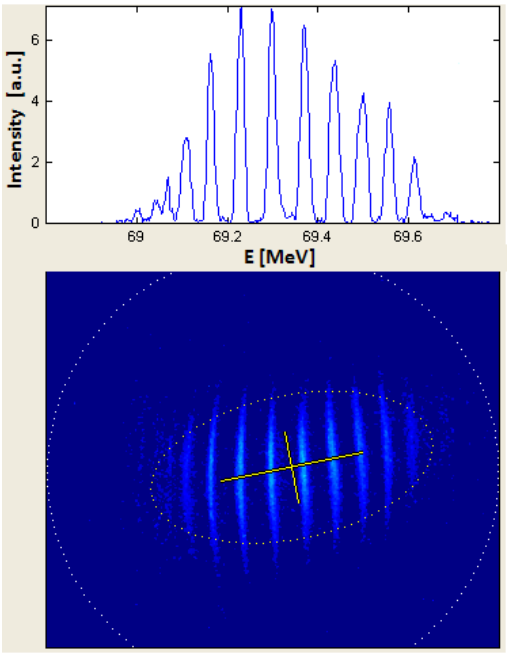

FIG. 3: The zero phasing of the compressed 90 pC beam. The BC compression factor is 2.5. The horizontal axis gives spectrometer readings in MeV. The vertical axis shows amplitude in arbitrary units.

of 2. The substructures of these sizes are easily detected by the SDL longitudinal diagnostics described above.

Subsequently, we compress the modulated electron beam and then perform zero-phasing measurement with accelerating section 4 after removing the residual energy chirp with section 3. The smallest modulation amplitude resolvable by the SDL spectrometer is about 2-3%. Therefore, the maximum gain that can be measured reliably with this setup is about 40. This sets the limit on the BC compression ratio that can be used in the experiment. In our studies, we chose a 2.5 compression factor. Fig. 3 illustrates the result of the described measurement performed for the beam from Fig. 2. As is evident, the microbunching instability dramatically increases the modulation of the compressed beam.

As follows from Eq. 4, for the chosen method of modulation of the photocathode laser, the bunch length changes with the frequency of modulation. Since we rely on the zero-phasing measurements to determine the latter parameter and the bunch length, obtaining a bunch with a specific current and modulation frequency would be a lengthy iterative process. Instead, we used the bunches of several charges modulated with various frequencies and amplitudes. This approach provided sets of data covering the gain curves for the range of currents, a procedure that is adequate for benchmarking of the model of microbunching instability.

Fig. 4 compares the results of directly measuring microbunching gain with the theoretical predictions given by Eq. 1. The error bars at high gain values are mostly driven by shot-to-shot variations; at low gain, the error is determined both by these variations and the background noise described above. The error bars in Fig. 4 result from propagation of the rms errors of the modulation amplitude of compressed and uncompressed beams, each measured for ten shots. We observed a good quantitative agreement between the experimental results and the theoretical predictions for the whole range of theory applicability.

Moreover, our data extend to even longer wavelengths than the ones where the theory still works. For instance, at both 220 μm and 240 μm modulation wavelengths become comparable with the length of the beam ($\sigma_z/\lambda = 1$ and 0.8, respectively, for 220 μm and 240 μm; we believe that $\sigma_z >> \lambda$ is a more accurate description of the Eq. 1 validity range than the constraint $k\sigma_z >> 1$ that we originally used in [15]), so the theory is not applicable in that region. There the measured gain quickly drops to about 2, thus limiting the bandwidth of the microbunching amplification at low frequencies.

Having confirmed the predictions of microbunching instability theory we now discuss the results of our measurements from a different perspective. Since the same mechanism that causes microbunching instability can be viewed as the LSC amplifier our results provide the first proof of principle demonstration of an LSCA. Others suggested [18] that several LSCA cascades, each consisting of

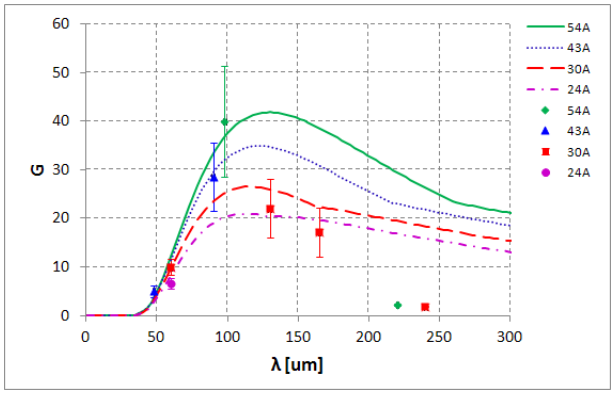

FIG. 4: Comparison of the direct measurement of microbunching gain and the theoretical predictions. Horizontal axis shows the modulation wavelength of the uncompressed beam. The vertical axis shows the microbunching gain. The symbols represent the experimental data (green diamonds correspond to the 54 A current, blue triangle shows the 43 A current, red squares and pink circles respectively represent the 30 A and 24 A currents). The lines depict the theoretical curves for the microbunching gain (green solid line corresponds to the 54 A current, blue dotted line shows the 43 A current, red dashed and pink dash-dot lines, respectively, represent the 30 A and 24 A currents)

the focusing channel followed by a chicane, can be combined to produce a pre-modulated beam for the FEL. Our experiment clearly demonstrates the feasibility of LSCA idea.

We have a single-stage LSCA, which starts with a coherently seeded electron beam. The amplifier we tested could be very useful for enhancing the tunability of linac-based multicycle THz sources. One example of such sources, is the source [14], first developed at the SDL, that generates tunable, narrow-band few-cycle and multicycle coherent THz radiation by intercepting the modulated electron beam with an aluminum mirror. Although a higher charge per bunch is desirable for strong THz radiation, it fundamentally is limited by the space charge effects at low energy, which also set the upper limit to the modulation frequency of the electron beam. It was shown [14] that the practical limit for modulation wavelength is about 115 μm at 100 pC beam charge.

This limitation might well be overcome by applying LSCA to considered THz source. Indeed, our results demonstrate the 100% density modulation at 24 μm wavelength for 120 pC beam and 38 μm for 250 pC beam.

Furthermore, we believe that other methods of producing density modulated beams for generation of narrow band THz radiation [19–27] might benefit from the application of demonstrated LSCA, since it increases both the charge and the modulation frequency available to the linac-based tunable few-cycle and multicycle THz sources.

In conclusion, we performed the first systematic studies of microbunching instability. By comparing the pre-modulated electron beams with the unmodulated ones before and after the compression we, for the first time, directly measured the microbunching gain. Our results showed good quantitative agreement with theoretical predictions.

In addition, our experiment provides the first demonstration of the LSCA. We show that the particular LSCA can be applied to significant enhancement of the linac-based tunable few-cycle and multicycle coherent THz sources.

We would like to thank G. L. Carr and G. Rakowsky for critical reading of the manuscript. We are grateful for support from the NSLS team. This work was supported in part by the U.S. Department of Energy under contract No. DE-AC02-98CH1-886.

[1] P. Emma et al., Nature Photonics 4, 641 - 647 (2010).
[2] J.B. Murphy and X.J. Wang, SRN, Vol. 21, No. 1, 41, 2008.
[3] S. Seletskiy et al., Phys. Rev. ST Accel. Beams 14, 110701 (2011).
[4] Z. Huang et al., Phys. Rev. ST Accel. Beams 13, 020703 (2010).
[5] M. Borland et al., Nucl. Instrum. Methods Phys. Res., Sect. A 483, 268 (2002).
[6] Z. Huang and K. Kim, Phys. Rev. ST Accel. Beams 5, 074401 (2002).
[7] E. Saldin, E. Schneidmiller and M. Yurkov, Nucl. Instrum. Methods Phys. Res., Sect. A 483, 516 (2002).
[8] S. Heifets, S. Krinsky and G. Stupakov, Phys.Rev. ST Accel. Beams 5, 064401 (2002).
[9] M. Venturini, Phys. Rev. ST Accel. Beams 11, 034401 (2008).
[10] E. Saldin, E. Schneidmiller, and M. Yurkov, Nucl. Instrum. Meth. A 528, 355 (2004).
[11] Z. Huang et al., Phys. Rev. ST Accel. Beams 7, 074401 (2004).
[12] S. Di Mitri, M. Cornacchia, S. Spampinati and S. Milton, Phys.Rev. ST Accel. Beams 13, 010702 (2010).
[13] M. Dohlus et al., Phys. Rev. ST Accel. Beams 14, 090702 (2011).
[14] Y. Shen et al., Phys. Rev. Lett. 107, 204801 (2011).
[15] S. Seletskiy et al., Proceedings of IPAC12, New Orleans, USA, 2012, TUPPP090.
[16] A. S. Weling et al., Appl. Phys. Lett. 64, 137 (1994).
[17] J. G. Neumann et al. J. Appl. Phys. 105, 053304 (2009).
[18] E.A. Schneidmiller and M.V. Yurkov, Phys. Rev. ST Accel. Beams 13, 110701 (2010).
[19] P. Muggli et al., Phys. Rev. Lett. 101, 054801 (2008).
[20] N. Kumar et al., Phys. Rev. Lett. 104, 255003 (2010).
[21] S. Bielawski et al., Nature Phys. 4, 390 (2008).
[22] M. Dunning et al., Phys. Rev. Lett. 109, 074801 (2012).

[23] Y.-E Sun et al., Phys. Rev. Lett. 105, 234801 (2010).
[24] P. Piot et al., Phys. Rev. ST Accel. Beams 14, 022801 (2011).
[25] D. Xiang and A. Chao, Phys. Rev. ST Accel. Beams 14, 114001 (2011).
[26] P. Musumeci et al., Phys. Rev. Lett. 106, 184801 (2011).
[27] K.L.F. Bane and G. Stupakov, Nucl. Instrum. Meth. A 677, (2012).